New Journal and we have not received input yet 23 (2021) 100926

Contents lists available at ScienceDirect

Thermal Science and Engineering Progress

journal homepage: www.sciencedirect.com/journal/thermal-science-and-engineering-progress

Guiding temperature waves with graded metamaterials

Zeren Zhang [a], Liujun Xu [a,*], Xiaoping Ouyang [b,*], Jiping Huang [a,*]

[a] Department of Physics, State Key Laboratory of Surface Physics, and Key Laboratory of Micro and Nano Photonic Structures (MOE), Fudan University, Shanghai 200438, China

[b] School of Materials Science and Engineering, Xiangtan University, Xiangtan 411105, China

ARTICLE INFO

Keywords:
Temperature waveguides
Graded metamaterials
Convection-conduction systems

ABSTRACT

Temperature waves exist in many practical scenarios such as pulse heat sources and periodic temperature fluctuations, which have broad applications for thermal nondestructive detection. However, it is still challenging to guide temperature waves in irregularly shaped pipes because temperature waves might be strongly scattered. To solve the problem, we propose a scheme to guide temperature waves with graded metamaterials that have continuous parameter variations in space. Since graded metamaterials can ensure the same phases of thermal wavefronts despite different spatial distances, temperature waves can propagate in irregularly shaped pipes without scattering. We then demonstrate an elementary unit to realize the right-angle bending of temperature waves. Experimental suggestions are also provided to design the elementary unit with common materials and layered structures. We further combine the elementary units together to realize three practical functions including obstacle avoidance, thermal periscope, and reverse bending. These results have potential applications for thermal imaging and sensing in elbow pipes.

1. Introduction

Temperature waves refer to spatial propagations of periodic temperature fluctuations, which have been studied intensively in recent years. One mechanism of temperature waves is to modify the Fourier law with thermal relaxation, thus making the modified conduction equation hyperbolic [1–5]. Many structures were proposed to guide this type of temperature waves, such as crystals [6,7] and cloaks [8]. Another mechanism of temperature waves is to consider the Fourier law together with convection that has a hyperbolic feature. This type of temperature waves has also received broad attention [9–16] to reveal anti-parity-time symmetry [9–11] or design thermal cloaking [12–14]. Here, we care about temperature waves based on conduction and convection.

Since the proposal of transformation thermotics [17,18], temperature control with thermal metamaterials has made great achievements not only in conduction but also in convection and radiation [19,20]. A recent study proposed a cloak to manipulate heat fluxes and fluid flows simultaneously [21], which, however, focused on only steady states. Since temperature waves feature transient states and phase properties, it is still challenging to guide temperature waves in irregularly shaped pipes with existing thermal metamaterials. A major problem is that temperature waves might be strongly scattered and temperature information cannot be detected at output ports, which is unwanted for thermal detection [22–24]. Compared with guiding thermal conduction [25–30], scattering problem is especially serious for temperature waves because they have phase features, which makes artificial designs more complicated. Therefore, despite difficulty, guiding temperature waves is of practical value, especially for thermal detection.

Inspired by the research on wave bending in optics [31–34] or acoustics [35,36], we propose a scheme to guide temperature waves based on the transformation theory, which leads to anisotropic and inhomogeneous parameters. Since the coordinate transformation is quasi-conformal, we can remove the requirement of anisotropy. The rest requirement is inhomogeneity, which means parameters vary in space. Therefore, we can make use of graded metamaterials to realize the same effects [37]. We further perform finite-element simulations to confirm the theory and apply layered structures to realize the graded parameters. As model applications, we also design three practical functions including obstacle avoidance, thermal periscope, and reverse bending. Let us begin with the fundamental theory.

* Corresponding authors.
E-mail addresses: 13307110076@fudan.edu.cn (L. Xu), oyxp2003@aliyun.com (X. Ouyang), jphuang@fudan.edu.cn (J. Huang).

https://doi.org/10.1016/j.tsep.2021.100926

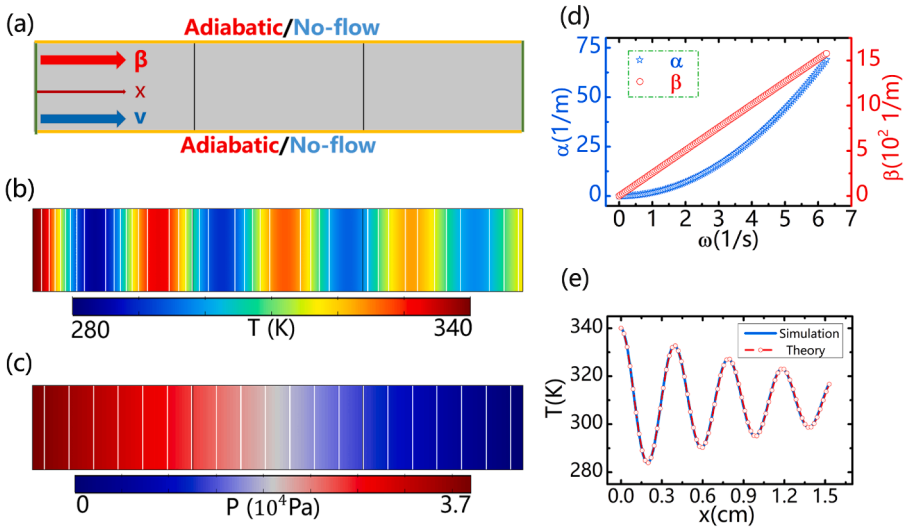

Fig. 1. Basic properties of temperature waves. (a) Schematic diagram of a rectangular temperature waveguide. The height and length of the left and right rectangles are $a = 2.25$ mm and $b = 5$ mm, and the middle rectangle is with length of $l = 3.5$ mm. (b) Temperature distribution and (c) pressure distribution at 20 s. White lines in (b) and (c) are isotherms and isobars, respectively. (d) Wave number as a function of ω. (e) Analytic and numerical temperature distributions. Parameters: $\sigma_s = 0.2$ W m^{-1} K^{-1}, $\rho_s = 1200$ kg/m^3, $C_s = 4000$ J kg^{-1} K^{-1}, $\phi = 0.7$, and $\eta = 1.5 \times 10^{-12}$ m^2 for the solid; $\sigma_f = 0.6$ W m^{-1} K^{-1}, $\rho_f = 1000$ kg/m^3, $C_f = 4200$ J kg^{-1} K^{-1}, and $\mu = 0.001$ Pa s for the fluid. $P_h = 3.7 \times 10^4$ Pa, $P_l = 10$ Pa, $A = 30$ K, $T_m = 310$ K, and $\omega = 2\pi$ rad/s. The initial temperature is 293 K.

2. Theory of temperature waves

Since we consider temperature waves based on conduction and convection, porous media are an ideal platform [38–40], which can flexibly control convection by tuning permeability. Therefore, we consider heat transfer in porous media, which is dominated by [41–47]

$$\rho_e C_e \partial T/\partial t + \nabla\cdot\left(-\sigma_e \nabla T + \rho_f C_f v T\right) = 0, \tag{1}$$

with $\rho_e C_e = \phi\rho_f C_f + (1-\phi)\rho_s C_s$ and $\sigma_e = \phi\sigma_f + (1-\phi)\sigma_s$. ρ_f (ρ_s), C_f (C_s), and σ_f (σ_s) are the mass density, heat capacity, and thermal conductivity of a fluid (solid), respectively. ϕ is the porosity of a solid. The Peclet number (defined as $\mathrm{Pe} = vL/D$, where v is convective velocity, L is characteristic length, and D is thermal diffusivity) can help to compare convection and conduction. The chosen parameters lead to $\mathrm{Pe} \approx 450$, indicating that thermal convection dominates. Therefore, the system mainly exhibits hyperbolic features and propagating waves can be supported. The fluid velocity in porous media is dominated by the Darcy law [48], i.e., $v = -(\eta/\mu)\nabla P$, where η is permeability, μ is dynamic viscosity, and P represents pressure. The chosen parameters also lead to $v \approx 4$ mm/s, which satisfies the hypothesis of the Darcy law.

We then consider a rectangular waveguide where a temperature wave propagates along the x axis, as shown in Fig. 1(a). The left boundary is set with a harmonic temperature [i.e., $T_h = A\cos(\omega t) + T_m$, where A is temperature amplitude, ω is circular frequency, and T_m is reference temperature] and a high pressure. The right boundary is set as an open boundary with a low pressure. The upper and lower boundaries are adiabatic and no-flow. The temperature wave can be mathematically expressed as

$$T = A\mathrm{e}^{\mathrm{i}(\gamma x - \omega t)} + T_m, \tag{2}$$

where γ is wave number. Only the real part of Eq. (2) makes sense, referring to a periodic temperature profile in space and time. Since we preset an incident frequency ω, the temperature amplitude decreases along the propagating direction. Therefore, Eq. (2) can also be denoted as $T = A\mathrm{e}^{-\alpha x}\mathrm{e}^{\mathrm{i}(\beta x - \omega t)} + T_m$, where we suppose that the γ in Eq. (2) to be complex, i.e., $\gamma = \beta + \mathrm{i}\alpha$. The imaginary part of γ refers to the spatial decay rate of a temperature wave. The temperature and pressure distributions are presented in Fig. 1(b) and (c), respectively. Clearly, the temperature wave dissipates when propagating from left to right. To obtain the wave number, we then substitute the trial solution into Eq. (1) to derive

$$\alpha = \frac{-2\rho_f C_f v + \sqrt{2}\epsilon}{4\sigma_e}, \tag{3a}$$

$$\beta = \frac{\sqrt{2}\epsilon^3 - 2\sqrt{2}\left(\rho_f C_f v\right)^2 \epsilon}{16\rho_e C_e \sigma_e^2 \omega}, \tag{3b}$$

with $\epsilon = \sqrt{\left(\rho_f C_f v\right)^2 + \sqrt{\left(\rho_f C_f v\right)^4 + 16(\rho_e C_e)^2 \sigma_e^2 \omega^2}}$. The physical meanings of α and β are the spatial decay rate and the wave number of a temperature wave, respectively. The $\alpha-\omega$ and $\beta-\omega$ curves are presented in Fig. 1(d), showing that higher frequencies yield larger spatial decay rates and wave numbers. Therefore, the propagation of temperature waves is influenced not only by transmission media but also by their own frequencies, which has an analog of optical dispersion. We also compare the theoretical calculations with the finite-element simulations performed by COMSOL Multiphysics (http://www.comsol.com/), and the results are shown in Fig. 1(e). Two identical lines indicate that the simulation result is in good agreement with the theoretical one. Therefore, the propagation of temperature waves in a rectangular waveguide is revealed and confirmed.

3. Right-angle bending of temperature waves

To guide temperature waves, we start from the transformation theory [42,13,49], whose main idea is to replace space transformations with material transformations. In this way, we can design a space transformation and then derive a corresponding material transformation, with transformed parameters $(\rho_e C_e)'$, σ_e', $(\rho_f C_f)'$, and v' expressed as

$$(\rho_e C_e)' = \frac{\rho_e C_e}{\det J}, \tag{4a}$$

$$\sigma_e' = \frac{J\sigma_e J^{\tau}}{\det J}, \tag{4b}$$

$$(\rho_f C_f)' = \rho_f C_f, \tag{4c}$$

$$v' = \frac{Jv}{\det J}, \tag{4d}$$

where J is the Jacobian transformation matrix, J^{τ} means the transpose of J, and $\det J$ denotes the determinant of J. We do not transform the

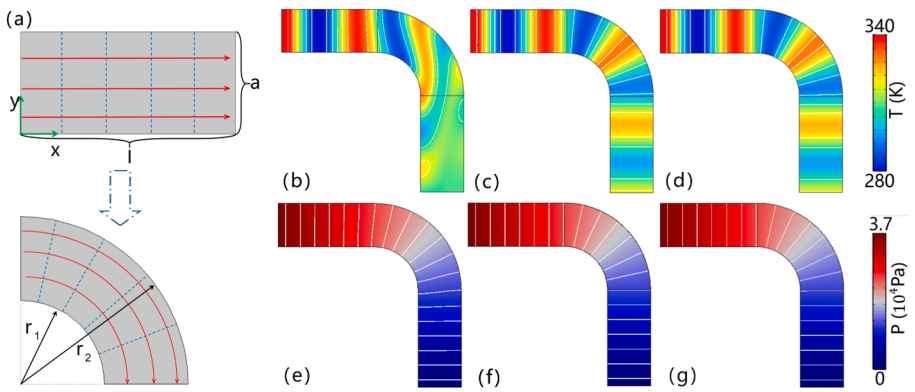

Fig. 2. Right-angle bending of temperature waves. (a) Schematic diagram of the coordinate transformation. (b)–(d) Temperature distributions and (e)–(g) pressure distributions at 20 s. In (b) and (e), the transformation theory is not applied, so parameters and boundary conditions are the same as those for Fig. 1. In (c) and (f), the transformation theory [Eqs. (8b) and (8c)] is applied. In (d) and (g), the graded parameters described by Eqs. (9a) and (9b) are used. $r_1 = 2.25$ mm and $r_2 = 4.5$ mm. Other parameters are the same as those for Fig. 1.

parameters of fluids because it is more difficult to control fluids than solids. Therefore, by considering the weighed average and the Darcy law, we can reduce Eq. (4) to

$$(\rho_s C_s)' = \frac{(\rho_e C_e)' - \phi\rho_f C_f}{1-\phi}, \tag{5a}$$

$$\sigma_s' = \frac{\sigma_e' - \phi\sigma_f}{1-\phi}, \tag{5b}$$

$$\eta' = \frac{J\eta J^{\tau}}{\det J}. \tag{5c}$$

Eq. (5) gives the transformation rule for solids, so we can control temperature waves at will in principle.

We then discuss a coordinate transformation to realize the right-angle bending of temperature waves. For this purpose, the middle part of a rectangular waveguide is bent as schematically shown in Fig. 2(a). The coordinate transformation can be mathematically expressed as

$$r = (r_2 - r_1)y/a + r_1, \tag{6a}$$

$$\theta = \pi(l-x)/(2l), \tag{6b}$$

where (r,θ) represents the cylindrical coordinates in the physical space, and (x,y) denotes the rectangular coordinates in a virtual space. In a virtual space, parameters are not transformed, and temperature control results from a space transformation. However, in the physical space, parameters are transformed according to transformation rules [Eq. (5)]. Therefore, the key to the transformation theory is to replace a space transformation with a parameter transformation, so phenomena in a virtual space can also be realized by transforming parameters in the physical space. We can then get the Jacobian transformation matrix J as

$$J = \begin{bmatrix} 0 & (r_2 - r_1)/a \\ -r\pi/(2l) & 0 \end{bmatrix} = \begin{bmatrix} 0 & 1 \\ -r\pi/(2l) & 0 \end{bmatrix}. \tag{7}$$

with $\xi = 1/\det J = 2l/(r\pi)$. According to Eq. (5), the transformed parameters can be expressed as

$$(\rho_s C_s)' = \frac{\rho_e C_e \xi - \phi\rho_f C_f}{1-\phi}, \tag{8a}$$

$$\sigma_s' = \begin{bmatrix} (\sigma_e\xi - \phi\sigma_f)/(1-\phi) & 0 \\ 0 & (\sigma_e/\xi - \phi\sigma_f)/(1-\phi) \end{bmatrix}, \tag{8b}$$

$$\eta' = \begin{bmatrix} \eta\xi & 0 \\ 0 & \eta/\xi \end{bmatrix}. \tag{8c}$$

where the thermal conductivity and permeability are anisotropic and inhomogeneous.

The propagation of thermal waves in a right-angle bending waveguide is presented in Fig. 2(b) and (e), where parameters are not transformed. Obviously, the temperature wave is strongly distorted due to scattering [see Fig. 2(b)], which is unwanted for thermal detection. Meanwhile, the pressure profile is no longer linear though it is not distorted as seriously as the temperature profile [see Fig. 2(e)]. This is because the pressure profile is dominated by a diffusion process where phases are not important. However, temperature waves feature phase properties. The temperature waves in the outer pipe go through longer spatial distances than those in the inner pipe, so the phases of thermal wavefronts in the curved part are no longer consistent. Therefore, the curved pipe does not affect the pressure profile strongly but distorts the temperature wave seriously. This is also why guiding temperature waves is important but difficult.

To remove distortion, we design the parameters as required by Eq. (8), and the results are shown in Fig. 2(c) and (f). The temperature wave can propagate smoothly with transformed parameters and the pressure profile also becomes linear, which consists with the results in Fig. 1(b) and (c). Therefore, the transformation scheme does work. The capability can be attributed to phase compensation with transformed parameters. The phases of thermal wavefronts can thus be kept the same in the curved part, so temperature propagation does not have scattering.

Although we have successfully guided temperature waves without disturbance, the parameters, such as thermal conductivity and permeability [Eqs. (8b) and (8c)], are still anisotropic. If we can further remove the requirement of anisotropy, the scheme can be more feasible for practical applications. For this purpose, we analyze the propagation features of temperature waves. Actually, since the radial component of a tensorial parameter has no effect on thermal wave propagation, an isotropic material is enough to realize the same effects. We then reduce Eqs. (8b) and (8c) to graded parameters by only keeping their tangential components,

$$\sigma_s' = (\sigma_e/\xi - \phi\sigma_f)/(1-\phi), \tag{9a}$$

$$\eta' = \eta/\xi, \tag{9b}$$

where the thermal conductivity and permeability are inhomogeneous but without anisotropy. Meanwhile, the parameters described by Eq. (9) increase as r increases, indicating larger values in the outer pipe. A larger thermal conductivity brings about a larger heat transfer efficiency, and a larger permeability leads to a larger convective velocity. Since phase mismatch is attributed to different spatial distances, larger parameters in the outer pipe can speed up the wave propagation in the outer pipe. Therefore, phase mismatch can be avoided in the curved part despite different spatial distances. The results based on Eqs. (9a) and (9b) are presented in Fig. 2(d) and (g), following the same patterns as Fig. 2(c) and (f). Therefore, graded metamaterials are sufficient to achieve the right-angle bending of temperature waves.

Furthermore, we discrete the graded metamaterial into N-layer homogenous materials to provide convenience for experiments. The operation makes the layer number or thickness crucial [50,51].

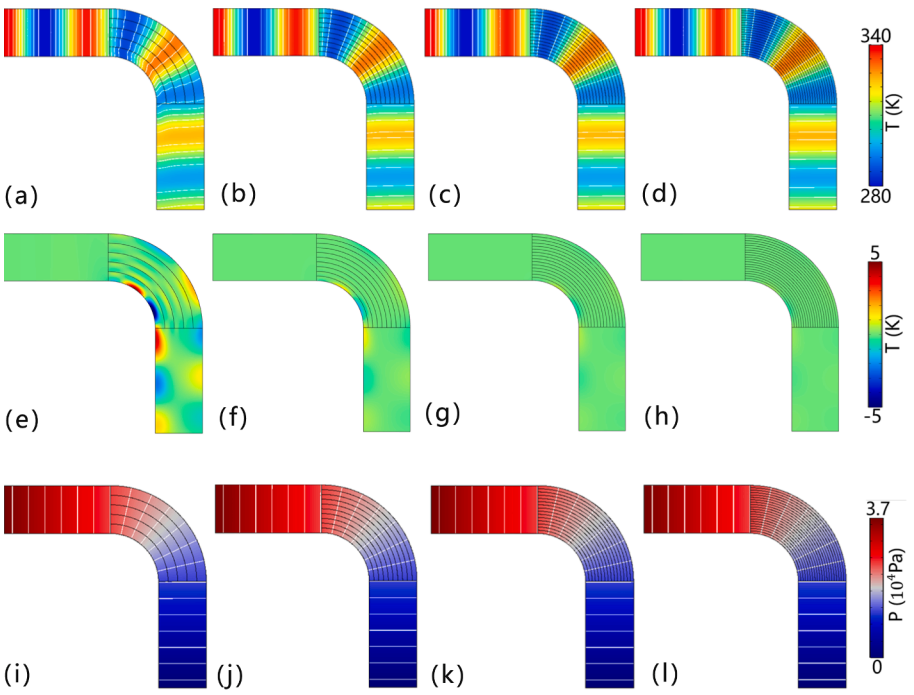

Fig. 3. Practical designs for Fig. 2 with layered structures. Each layer has isotropic and homogeneous parameters, obtained by taking the middle coordinate into Eqs. (9a) and (9b). (a)–(d) Temperature distributions, (e)–(h) temperature distributions in (a)-(d) minus those with ideal parameters, and (i)–(l) pressure distributions with 5, 10, 15, and 20 layers at 20 s, respectively.

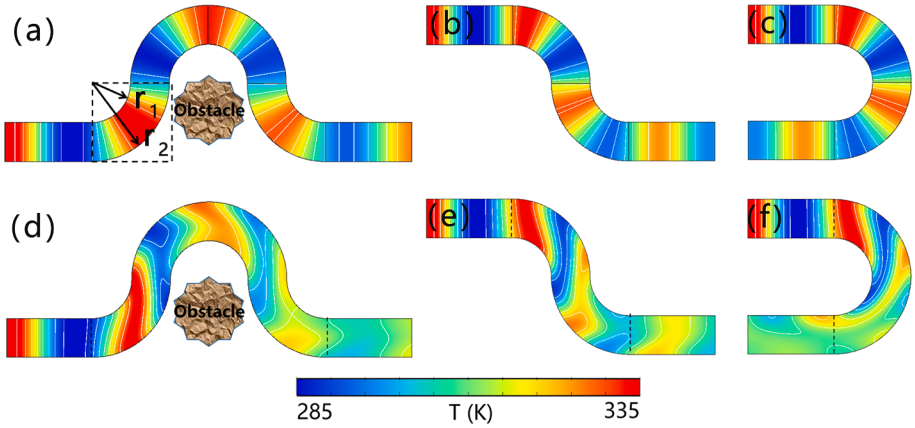

Fig. 4. Practical applications of right-angle bending. (a) Obstacle avoidance. (b) Thermal periscope. (c) Reverse bending. (d)–(f) Comparisons without applying graded metamaterials. The dashed square in (a) can be treated as an elementary unit, whose parameters are the same as those in Fig. 2.

Therefore, we study the effect of different layer numbers on the performance of temperature waveguide. The parameters of each layer can be obtained by taking the corresponding middle coordinate into Eqs. (9a) and (9b). As shown in Fig. 3, the first and third rows present the temperature and pressure distributions (from left to right) with 5, 10, 15, and 20 layers at 20 s, respectively. The second row shows the temperature profiles with layered structures minus those with ideal parameters at 20 s. Clearly, more layers perform better because parameters are closer to theoretical values. With the increment of layer numbers from 10 to 20, the improved effect is no longer obvious, so 20 layers are efficient enough.

4. Practical applications

With the elementary unit of right-angle bending, we are able to find more realistic applications by combining the elementary units together appropriately. For instance, when a barrier hinders the propagation of temperature waves, we can design a temperature waveguide shown in Fig. 4(a) to make a temperature wave bypass the barrier. Compared with Fig. 4(d) where a temperature wave is strongly distorted, the obstacle avoidance can ensure smooth propagation of a temperature wave. Moreover, it is indispensable for a submarine to equip a periscope, but most periscopes are optical, which may limit detective efficiency at dark regions. So the idea for thermal periscope may broaden detection ranges. Fig. 4(b) is a demo for thermal periscopes. Compared with Fig. 4 (e) which has not any design, thermal periscopes do detect temperature information as expected. We finally present the application of reverse bending in Fig. 4(c), and Fig. 4(f) shows the result without performing transformation. These results show that the right-angle bending of temperature waves is flexible to design various extended devices, which have broad applications for thermal management.

We also provide some experimental suggestions to ensure completeness. When performing simulations, we choose water as fluids, and solids can be porous rocks or aerogel [38–40]. The input

temperature wave can be generated by using a periodic temperature source, such as a pulse heat source. The detection of temperature waves can resort to an infrared camera. Therefore, these results should be validated experimentally in principle. These results have potential applications for thermal wave detection [22–24], thermal sensing [52–55], thermal camouflaging [56–64], etc.

5. Conclusion

In summary, we have proposed a scheme to guide temperature waves with graded metamaterials, which can compensate phase mismatch induced by different spatial distances. Therefore, temperature waves can propagate without distortion in a right-angle pipe. Although graded metamaterials feature continuous variations of parameters, they can be simplified by layered structures. We have also studied the effect of layer numbers on temperature propagation. Although more layers are better, 20 layers are enough to exhibit good performance. As model applications, we further propose three practical functions including obstacle avoidance, thermal periscope, and reverse bending. These results have potential applications for thermal detection in irregularly shaped pipes. Further explorations on temperature waves like wave splitters and wave shifters can be expected with the present scheme.

CRediT authorship contribution statement

Zeren Zhang: Formal analysis, Writing - original draft. **Liujun Xu:** Conceptualization, Writing - original draft. **Xiaoping Ouyang:** Conceptualization, Writing - original draft. **Jiping Huang:** Conceptualization, Writing - original draft.

Declaration of Competing Interest

The authors declare that they have no known competing financial interests or personal relationships that could have appeared to influence the work reported in this paper.

Acknowledgments

We acknowledge financial support from the National Natural Science Foundation of China under Grants Nos. 11725521 and 12035004, and from the Science and Technology Commission of Shanghai Municipality under Grant No. 20JC1414700.

References

[1] D.D. Joseph, L. Preziosi, Heat waves, Rev. Mod. Phys. 61 (1) (1989) 41–73.
[2] B.-D. Nie, B.-Y. Cao, Three mathematical representations and an improved ADI method for hyperbolic heat conduction, Int. J. Heat Mass Transfer 135 (2019) 974–984.
[3] M. Gandolfi, G. Benetti, C. Glorieux, C. Giannetti, F. Banfi, Accessing temperature waves: A dispersion relation perspective, Int. J. Heat Mass Transfer 143 (2019) 118553.
[4] M. Simoncelli, N. Marzari, A. Cepellotti, Generalization of Fourier's Law into viscous heat equations, Phys. Rev. X 10 (1) (2020) 011019.
[5] Y. Liu, L. Li, Y. Zhang, Numerical simulation of non-Fourier heat conduction in fins by lattice Boltzmann method, Appl. Therm. Eng. 166 (2020) 114670.
[6] A.-L. Chen, Z.-Y. Li, T.-X. Ma, X.-S. Li, Y.-S. Wang, Heat reduction by thermal wave crystals, Int. J. Heat Mass Transfer 121 (2018) 215–222.
[7] M. Gandolfi, C. Giannetti, F. Banfi, Temperonic crystal: A Superlattice for temperature waves in graphene, Phys. Rev. Lett. 125 (26) (2020) 265901.
[8] M. Farhat, S. Guenneau, P.-Y. Chen, A. Alù, K.N. Salama, Scattering cancellation-based cloaking for the Maxwell-Cattaneo heat waves, Phys. Rev. Appl. 11 (4) (2019) 044089.
[9] Y. Li, Y.-G. Peng, L. Han, M.-A. Miri, W. Li, M. Xiao, X.-F. Zhu, J. Zhao, A. Alù, S. Fan, C.-W. Qiu, Anti-parity-time symmetry in diffusive systems, Science 364 (2019) 170–173.
[10] P. Cao, Y. Li, Y. Peng, C. Qiu, X. Zhu, High-order exceptional points in diffusive systems: robust APT symmetry against perturbation and phase oscillation at APT symmetry breaking, ES Energy Environ. 7 (2020) 48–55.
[11] L. Xu, J. Wang, G. Dai, S. Yang, F. Yang, G. Wang, J. Huang, Geometric phase, effective conductivity enhancement, and invisibility cloak in thermal convection-conduction, Int. J. Heat Mass Transfer 165 (2021) 120659.
[12] M. Farhat, P.-Y. Chen, H. Bagci, C. Amra, S. Guenneau, A. Alù, Thermal invisibility based on scattering cancellation and mantle cloaking, Sci. Rep. 5 (2015) 9876.
[13] L. Xu, J. Huang, Controlling thermal waves with transformation complex thermotics, Int. J. Heat Mass Transfer 159 (2020) 120133.
[14] L.-J. Xu, J.-P. Huang, Active thermal wave cloak, Chin. Phys. Lett. 37 (2020) 120501.
[15] L. Xu, J. Huang, Thermal convection-diffusion crystal for prohibition and modulation of wave-like temperature profiles, Appl. Phys. Lett. 117 (1) (2020) 011905.
[16] L. Xu, J. Huang, Negative thermal transport in conduction and advection, Chin. Phys. Lett. 37 (2020) 080502.
[17] C.Z. Fan, Y. Gao, J.P. Huang, Shaped graded materials with an apparent negative thermal conductivity, Appl. Phys. Lett. 92 (2008) 251907.
[18] T. Chen, C.-N. Weng, J.-S. Chen, Cloak for curvilinearly anisotropic media in conduction, Appl. Phys. Lett. 93 (2008) 114103.
[19] J. Wang, G. Dai, J. Huang, Thermal metamaterial: Fundamental, application, and outlook, iScience 23 (10) (2020) 101637.
[20] J.-P. Huang, Theoretical Thermotics: Transformation Thermotics and Extended Theories for Thermal Metamaterials, Springer, Singapore, 2020.
[21] B. Wang, T.-M. Shih, J. Huang, Transformation heat transfer and thermo-hydrodynamic cloaks for creeping flows: manipulating heat fluxes and fluid flows simultaneously, Appl. Therm. Eng. 190 (2021) 116726.
[22] R. Mulaveesala, S. Tuli, Theory of frequency modulated thermal wave imaging for nondestructive subsurface defect detection, Appl. Phys. Lett. 89 (19) (2006) 191913.
[23] R. Mulaveesala, S. Tuli, Applications of frequency modulated thermal wave imaging for non-destructive characterization, AIP Conf. Proc. 1004 (1) (2008) 15.
[24] S. Tuli, K. Chatterjee, Frequency modulated thermal wave imaging, AIP Conf. Proc. 1430 (1) (2012) 523.
[25] K.P. Vemuri, P.R. Bandaru, Geometrical considerations in the control and manipulation of conductive heat flux in multilayered thermal metamaterials, Appl. Phys. Lett. 103 (13) (2013) 133111.
[26] T. Yang, K.P. Vemuri, P.R. Bandaru, Experimental evidence for the bending of heat flux in a thermal metamaterial, Appl. Phys. Lett. 105 (8) (2014) 083908.
[27] K.P. Vemuri, P.R. Bandaru, Anomalous refraction of heat flux in thermal metamaterials, Appl. Phys. Lett. 104 (8) (2014) 083901.
[28] F.M. Canbazoglu, K.P. Vemuri, P.R. Bandaru, Estimating interfacial thermal conductivity in metamaterials through heat flux mapping, Appl. Phys. Lett. 106 (14) (2015) 143904.
[29] R. Hu, B. Xie, J. Hu, Q. Chen, X. Luo, Carpet thermal cloak realization based on the refraction law of heat flux, EPL 111 (2015) 54003.
[30] R. Hu, S. Zhou, W. Shu, B. Xie, Y. Ma, X. Luo, Directional heat transport through thermal reflection meta-device, AIP Adv. 6 (12) (2016) 125111.
[31] A.M. Mahmoud, N. Engheta, Wave-matter interactions in epsilon-and-mu-near-zero structures, Nat. Commun. 5 (2014) 5638.
[32] H. Liu, X. Zhu, L. Liang, X. Zhang, Y. Yang, Tunable transformation optical waveguide bends in liquid, Optica 4 (8) (2017) 839–846.
[33] Y. Zhang, B. Zhang, Bending, splitting, compressing and expanding of electromagnetic waves in infinitely anisotropic media, J. Opt. 20 (2018) 014001.
[34] Y. Zuo, H. Liu, Y. Yang, Optofluidic waveguide bending by thermal diffusion for visible light control, Opt. Lett. 45 (13) (2020) 3725.
[35] W. Lu, H. Jia, Y. Bi, Y. Yang, J. Yang, Design and demonstration of an acoustic right-angle bend, J. Acoust. Soc. Am. 142 (1) (2017) 84.
[36] G.-S. Liu, Y. Zhou, M.-H. Liu, Y. Yuan, X.-Y. Zou, J.-C. Cheng, Acoustic waveguide with virtual soft boundary based on metamaterials, Sci. Rep. 10 (2020) 981.
[37] Y. Xu, Y. Fu, H. Chen, Planar gradient metamaterials, Nat. Rev. Mater. 1 (2016) 16067.
[38] Z.G. Qu, Y.D. Fu, Y. Liu, L. Zhou, Approach for predicting effective thermal conductivity of aerogel materials through a modified lattice Boltzmann method, Appl. Therm. Eng. 132 (2018) 730–739.
[39] M.H. Esfe, M. Bahiraei, H. Hajbarati, M. Valadkhani, A comprehensive review on convective heat transfer of nanofluids in porous media: Energy-related and thermohydraulic characteristics, Appl. Therm. Eng. 178 (2020) 115487.
[40] G.S.S. Prabha, M.C. Bharathi, R.B. Kudenatti, Heat transfer through mixed convection boundary layer in a porous medium: LTNE analysis, Appl. Therm. Eng. 179 (2020) 115705.
[41] J. Bear, M.Y. Corapcioglu, Fundamentals of Transport Phenomena in Porous Media, Springer, 1984.
[42] G. Dai, J. Shang, J. Huang, Theory of transformation thermal convection for creeping flow in porous media: cloaking, concentrating, and camouflage, Phys. Rev. E 97 (2) (2018) 022129.
[43] F.B. Yang, L.J. Xu, J.P. Huang, Thermal illusion of porous media with convection-diffusion process: transparency, concentrating, and cloaking, ES Energy Environ. 6 (2019) 45–50.
[44] W.-S. Yeung, V.-P. Mai, R.-J. Yang, Cloaking: Controlling thermal and hydrodynamic fields simultaneously, Phys. Rev. Appl. 13 (6) (2020) 064030.
[45] L. Xu, J. Huang, Chameleonlike metashells in microfluidics: A passive approach to adaptive responses, Sci. China-Phys. Mech. Astron. 63 (2) (2020) 228711.
[46] D. Huu-Quan, A.M. Rostami, M.S. Rad, M. Izadi, A. Hajjar, Q. Xiong, 3D numerical investigation of turbulent forced convection in a double-pipe heat exchanger with flat inner pipe, Appl. Therm. Eng. 182 (2021) 116106.
[47] L.B. Tomanek, D.S. Stutts, Material thermal properties estimation via a one-dimensional transient convection model, Appl. Therm. Eng. 184 (2021) 116362.
[48] Y.A. Urzhumov, D.R. Smith, Fluid flow control with transformation media, Phys. Rev. Lett. 107 (7) (2011) 074501.

[49] S. Guenneau, D. Petiteau, M. Zerrad, C. Amra, T. Puvirajesinghe, Transformed fourier and fick equations for the control of heat and mass diffusion, AIP Adv. 5 (5) (2015) 053404.
[50] M. Ghaneifar, H. Arasteh, R. Mashayekhi, A. Rahbari, R.B. Mahani, P. Talebizadehsardari, Thermohydraulic analysis of hybrid nanofluid in a multilayered copper foam heat sink employing local thermal non-equilibrium condition: Optimization of layers thickness, Appl. Therm. Eng. 181 (2020) 115961.
[51] R. Hu, S. Iwamoto, L. Feng, S. Ju, S. Hu, M. Ohnishi, N. Nagai, K. Hirakawa, J. Shiomi, Machine-Learning-Optimized Aperiodic Superlattice Minimizes Coherent Phonon Heat Conduction, Phys. Rev. X 10 (2) (2020) 021050.
[52] T. Yang, X. Bai, D. Gao, L. Wu, B. Li, J.T.L. Thong, C.-W. Qiu, Invisiable sensor: Simultaneous camouflaging and sensing in multiphysical fields, Adv. Mater. 27 (47) (2015) 7752.
[53] T. Han, P. Yang, Y. Li, D. Lei, B. Li, K. Hippalgaonkar, C.-W. Qiu, Full-parameter omnidirectional thermal metadevices of anisotropic geometry, Adv. Mater. 30 (49) (2018) 1804019.
[54] P. Jin, L. Xu, T. Jiang, L. Zhang, J. Huang, Making thermal sensors accurate and invisible with an anisotropic monolayer scheme, Int. J. Heat Mass Transfer 163 (2020) 120437.
[55] L. Xu, J. Huang, T. Jiang, L. Zhang, J. Huang, Thermally invisible sensors, EPL 132 (2020) 14002.
[56] R. Hu, S. Zhou, Y. Li, D.-Y. Lei, X. Luo, C.-W. Qiu, Illusion thermotics, Adv. Mater. 30 (22) (2018) 1707237.
[57] J. Guo, Z.G. Qu, Thermal cloak with adaptive heat source to proactively manipulate temperature field in heat conduction process, Int. J. Heat Mass Transfer 127 (2018) 1212–1222.
[58] Y. Li, K.-J. Zhu, Y.-G. Peng, W. Li, T. Yang, H.-X. Xu, H. Chen, X.-F. Zhu, S. Fan, C.-W. Qiu, Thermal meta-device in analogue of zero-index photonics, Nat. Mater. 18 (2019) 48–54.
[59] R. Hu, S. Huang, M. Wang, X. Luo, J. Shiomi, C.-W. Qiu, Encrypted thermal printing with regionalization transformation, Adv. Mater. 31 (25) (2019) 1807849.
[60] L.J. Xu, S. Yang, J.P. Huang, Effectively infinite thermal conductivity and zero-index thermal cloak, EPL 131 (2020) 24002.
[61] J. Li, Y. Li, P.-C. Cao, T. Yang, X.-F. Zhu, W. Wang, C.-W. Qiu, A continuously tunable solid-Like convective thermal metadevice on the reciprocal line, Adv. Mater. 32 (42) (2020) 2003823.
[62] L. Xu, X. Zhao, Y. Zhang, J. Huang, Tailoring dipole effects for achieving thermal and electrical invisibility simultaneously, Eur. Phys. J. B 93 (2020) 101.
[63] J. Guo, Z. Qu, X. Wang, A reverse thermal cloak design method based on inverse problem theory, ES Energy Environ. 7 (2020) 71–83.
[64] R. Hu, W. Xi, Y. Liu, K. Tang, J. Song, X. Luo, J. Wu, C.-W. Qiu, Thermal camouflaging metamaterials, Mater. Today, in press. doi: 10.1016/j.mattod.2020.11.013.